The Canadian Mineralogist
Vol. 52, pp. 653-670 (2014)
DOI: 10.3749/canmin.1400006

THE MINERALOGY, GEOCHEMISTRY, AND METALLURGY OF COBALT IN THE RHOMBOHEDRAL CARBONATES

ISABEL F. BARTON[§]

Lowell Institute for Mineral Resources, University of Arizona, Tucson, AZ 85721

HEXIONG YANG

Department of Geosciences, University of Arizona, 1040 4th St, Tucson, AZ 85721

MARK D. BARTON

Department of Geosciences, University of Arizona, 1040 4th St, Tucson, AZ 85721 and Lowell Institute for Mineral Resources, University of Arizona, 1235 E. James E. Rogers Way, Tucson, AZ 85721

ABSTRACT

Carbonate ores of cobalt are a significant but under-recognized fraction of the global Co resource. Cobalt forms spherocobaltite ($CoCO_3$, calcite group), whose complete solid solution with isostructural magnesite, $MgCO_3$, is described here for the first time. Cobalt-rich dolomite, $Ca(Mg,Co)(CO_3)_2$, and Co-rich calcite, $(Ca,Co)CO_3$, can accommodate up to 20 mol.% Co and up to 2 mol.% Co, respectively. Cobalt has also been reported as a minor substituent of other calcite-group carbonates and as a major constituent of the non-rhombohedral carbonates comblainite, $Ni_4Co^{3+}_2(OH)_{12}(CO_3)\cdot 3H_2O$ (hydrotalcite supergroup), and kolwezite, $(Cu,Co)_2(CO_3)(OH)_2$ (poorly understood, possibly rosasite group).

Cobalt carbonates are most common in the supergene zones of Cu-Co sulfide ore deposits, especially the Central African Copperbelt. A study focused on the Tenke-Fungurume district (TFM) in the Copperbelt found Co-rich dolomite, Co-rich magnesite, spherocobaltite, and kolwezite. Cobalt-rich dolomite occurs as Co-rich bands in supergene dolomite and as individual Co-rich dolomite crystals filling void spaces. Members of the magnesite-spherocobaltite solid solution occur as crystals filling void spaces in rocks and as microscopic inclusions with kolwezite in supergene chalcocite (Cu_2S) replacing primary carrollite ($CuCo_2S_4$).

The formation of Co-rich carbonates remains enigmatic. Evidence from Bou Azzer indicates that they can form under specific hypogene conditions, but in general Co-rich carbonates form from supergene processes. Dedolomitization has been proposed as a mechanism of formation for the analogous Zn carbonates, but there is no evidence of dedolomitization in the TFM cobalt carbonates. Most of them appear to have precipitated directly from pockets of Co-(Mg)-(Cu)-carbonate-enriched solution trapped within oxidizing hypogene sulfides.

Cobalt carbonates pose a serious metallurgical problem. Most carbonate ores are processed by solvent extraction using acid. Solubility calculations indicate that the Co in carbonates is less soluble than Mg, Fe, and Ca by 3 to 4 orders of magnitude. Thus, acid leaching will liberate all other ions from carbonate ores before releasing appreciable Co. Furthermore, many of the Mg-rich spherocobaltites in this study were initially misidentified as Co-rich dolomite, which is far more soluble than spherocobaltite. This may cause Co recoveries to be lower than predicted at many Central African Copperbelt mines.

Keywords: magnesite, spherocobaltite, Co-rich dolomite, Copperbelt, carbonates, cobalt metallurgy.

[§] *Corresponding author e-mail address:* fay1@email.arizona.edu

Introduction

Cobalt worldwide

Cobalt is a strategic metal used in high-temperature steels, magnets, lithium-ion batteries, and other industrial applications. It also has medical uses: cobalt is the central atom in vitamin B12 (cobaltamine), and radioactive Co^{60} is the chief radiation source in cancer therapies.

The world's identified Co resource totals about 15 million metric tons, most of which is accessory in Ni-laterite deposits (Shedd 2013). Historical production has come chiefly from mafic- and ultramafic-hosted PGE deposits in Russia and Australia, but in recent years the Congolese deposits of the Central African Copperbelt have come to produce more than half the annual global supply of cobalt (Shedd 2013). Other contributions come from Příbram (Czech Republic), Tsumeb (Namibia), Bou Azzer (Morocco), the Flinders Range (Australia), and the Santa Rosalia district (Mexico) (Table 1).

Cobalt in rhombohedral carbonates

Crystal chemical factors determining cation substitution in carbonates

The carbonate structure consists of chains of cation coordination polyhedra sharing O ions. Thus, either each cation polyhedron must be of a shape and size to link up easily with its neighbors, or the neighboring polyhedra must distort to reach it. Highly distorted structures are unstable, so no carbonate can form unless its cation polyhedra require little distortion.

The formation of a stable, undistorted structure is most easily achieved in one-cation carbonates such as pure $CaCO_3$ or $FeCO_3$. In these, all the cation coordination polyhedra are the same size and shape and they do not have to distort to link into a chain. However, this is the ideal case: most naturally occurring carbonates contain multiple cation types, and each cation type has a different coordination polyhedron. If all the cation types have coordination polyhedra of similar shape and size, they can link to one another with very little distortion. In this case, the various cation types are distributed over the octahedral sites at random. This is the disordered or calcite structure, in which any cation present can occur at any cation site along the chain (Reeder 1983). But if the cation types have coordination polyhedra of very different sizes and shapes, they cannot link without distorting to a degree that makes the structure unstable. In this case, the carbonate must be stabilized by adopting the ordered or dolomite structure, in which the different cation types are sorted onto different, alternating sites. This alternation accommodates the necessary distortion by distributing it evenly over the chain of polyhedra, such that each polyhedron is stretched a little and none is stretched too much (Navrotsky & Loucks 1977).

Cobalt substitution in carbonates

In charge and ionic radius (0.745 Å), Co^{2+} is most similar to octahedral Mg^{2+} (0.72 Å), Fe^{2+} (0.78 Å),

TABLE 1. REPORTED OCCURRENCES OF COBALT CARBONATE MINERALS

Location	Reported species	Reference
Tenke-Fungurume, D.R. Congo	Magnesite-spherocobaltite, spherocobaltite, cobaltoan dolomite	This work
Przibram, Bohemia	Cobaltoan dolomite	Minceva-Stefanova 1997
Peramea, Spain	Cobaltoan calcite	Reeder *et al.* 1999
Durango, Colorado	Kolwezite	Daltry 1992
Kakanda, D.R. Congo	Cobaltoan dolomite, spherocobaltite	Gauthier & Deliens 1999
Mashamba West and Mindingi, D.R. Congo	Cobaltoan calcite	Gauthier & Deliens 1999
Tantara, D.R. Congo	Cobaltoan calcite	Gauthier & Deliens 1999
Kamoto, Musonoi, and Kabolela, D.R. Congo	Spherocobaltite, kolwezite	Gauthier & Deliens 1999; Pirard & Hatert 2008
Mupine, D.R. Congo	Spherocobaltite, cobaltoan calcite	Gauthier & Deliens 1999
Kambove, D.R. Congo	Cobaltoan dolomite Spherocobaltite	Van Langendonck *et al.* 2013; Gauthier & Deliens 1999
Konkola, Zambia	Cobaltoan dolomite	Sweeney *et al.* 1986
Chibuluma, Zambia	"Cobaltocalcite" – probably spherocobaltite	Whyte & Green 1971
Tsumeb, Namibia	Cobaltoan dolomite	Hurlbut 1957
Shinkolobwe, D.R. Congo	Comblainite	Daltry 1991

and Mn^{2+} (0.83 Å) (Shannon 1976). The Co^{2+} ion has a low-spin d^7 configuration and degeneracy in the t_{2g} orbital (Rosenberg & Foit 1979). Distorting the coordination octahedron removes the degeneracy, reducing the energy of the complex (Jahn-Teller effect). Thus, the Co^{2+} coordination octahedron is compressed relative to the Mg^{2+} octahedron (Rosenberg & Foit 1979). The Co-bearing carbonates stable in nature (Table 1) reflect these crystal-chemical factors.

Cobalt forms a stable calcite-structured carbonate (spherocobaltite, $CoCO_3$; also sphaerocobaltite or cobaltocalcite). Cobalt-rich calcite [$(Ca,Co)CO_3$] is also a recognized mineral, but it cannot contain much Co: Goldsmith & Northrop (1965) found a maximum of 15 mol.% Co in calcites at 800 °C, which dropped to less than 5 mol.% by 600 °C. Katsikopoulos *et al.* (2008) achieved 16 mol.% Co in low-temperature calcite only by dint of extreme Co-oversaturation in the fluid and mixture with silica gel. Such conditions are not very realistic in the supergene zones of ore deposits, where most Co-carbonates form. Simmonds (1980) observed calcites in the Central African Copperbelt with Co only up to 1.6 mol.%.

The transition metal carbonates have extensive solid solutions. The published analytical data for spherocobaltite solid solutions are scanty, but Clissold *et al.* (2003) detected minor Co in some gaspéite samples. Goldsmith & Northrop (1965) indicated a theoretical complete solid solution between spherocobaltite and magnesite at 600 °C and 15 kbar; this study is the first report of $(Mg,Co)CO_3$ in nature. The solid solutions of magnesite are better documented: magnesite has complete solid solutions with siderite at 250 °C (Anovitz & Essene 1987); with rhodochrosite at and above 500 °C and 10 kbar, and possibly at lower temperature (Goldsmith & Graf 1960); and with otavite at 800 °C and 1 GPa (Bromiley *et al.* 2007). At lower temperatures, however, a Cd-dolomite limits the extent of magnesite-otavite solid solution (Bromiley *et al.* 2007). Other partial solid solutions of magnesite include calcite (Goldsmith & Graf 1960, Mackenzie *et al.* 1983), gaspéite (Goldsmith & Northrop 1965), and smithsonite (Boni *et al.* 2011). However, there is no work up to the present on the magnesite-spherocobaltite solid solution below the conditions (600 °C and 15 kbar) at which Goldsmith & Northrop (1965) documented complete solid solution.

Cobalt does not form a stable dolomite-structured carbonate, either with other transition metal ions or with Ca^{2+}. All the transition metal ions, including Co^{2+}, have coordination octahedra of similar shape and size, so they can link into a chain with little distortion and have no need to assume any specific order (Reeder 1983). In the case of Ca^{2+}-rich dolomite-structured carbonates, the large Ca^{2+} ion is near the maximum size for octahedral coordination, and the Ca^{2+} polyhedron does not distort easily and will not form dolomite-structured carbonates with Co^{2+} and some of the other transition metals (Rosenberg & Foit 1979).

Cobalt may also occur in kolwezite [$(Cu,Co)_2(CO_3)(OH)_2$, rosasite group] and in comblainite [$Ni_4Co_2(OH)_{12}(CO_3)\cdot 3H_2O$, quintinite group]. Comblainite is notable as the only carbonate in which cobalt is trivalent. However, these are rare and poorly understood minerals, and their possible Co concentrations and even their crystal systems remain unconstrained (Perchiazzi & Merlino 2006, Frost *et al.* 2007). Calcite- and dolomite-group carbonates contain the world's entire economically significant Co carbonate resource.

This study began as part of a broader examination of the geology of the Tenke-Fungurume Cu-Co district (TFM) and other deposits on the Congolese side of the Central African Copperbelt. Research there includes work on the mineralogical controls on ore processing, so the metallurgy as well as the mineralogy of the ores are of interest to the overarching geological investigation.

Cobalt carbonates in the Central African Copperbelt

Overview: Geological background

The Central African Copperbelt of northern Zambia and southeastern D.R. Congo (Fig. 1) is one of the world's largest Cu and Co resources (Selley *et al.* 2005) and is a major source for Co-rich carbonate mineral specimens (Gauthier & Deliens 1999). Most Co-rich carbonates are produced during supergene alteration of cobalt sulfide ores, and the Co-carbonates of the Central African Copperbelt are no exception. The Co was originally a part of carrollite ($CuCo_2S_4$), which precipitated along with chalcopyrite ($CuFeS_2$), bornite (Cu_5FeS_4), and digenite (Cu_9S_5) in a Neoproterozoic basinal carbonate-clastic sequence (the Mines Series of the Roan Group, < 887 Ma; Cailteux 1994). Textural relationships are somewhat ambiguous but tend, overall, to indicate that carrollite precipitated before the Cu-Fe sulfides. However, all the sulfide ores seem to have precipitated during a single alteration episode sometime during diagenesis, accompanied by voluminous dolomitic alteration (Oosterbosch 1951, Schuh *et al.* 2012). Post-ore quartz replaced some of the dolomite. Further alteration occurred as thin-skinned Pan-African (570–510 Ma) deformation broke the mineralized rocks into separate "écailles" and pushed them northward into their present arcuate arrangement (Selley *et al.* 2005). Dating of the Copperbelt's large, coarsely crystalline, high-angle dolomite veins indicate that they formed

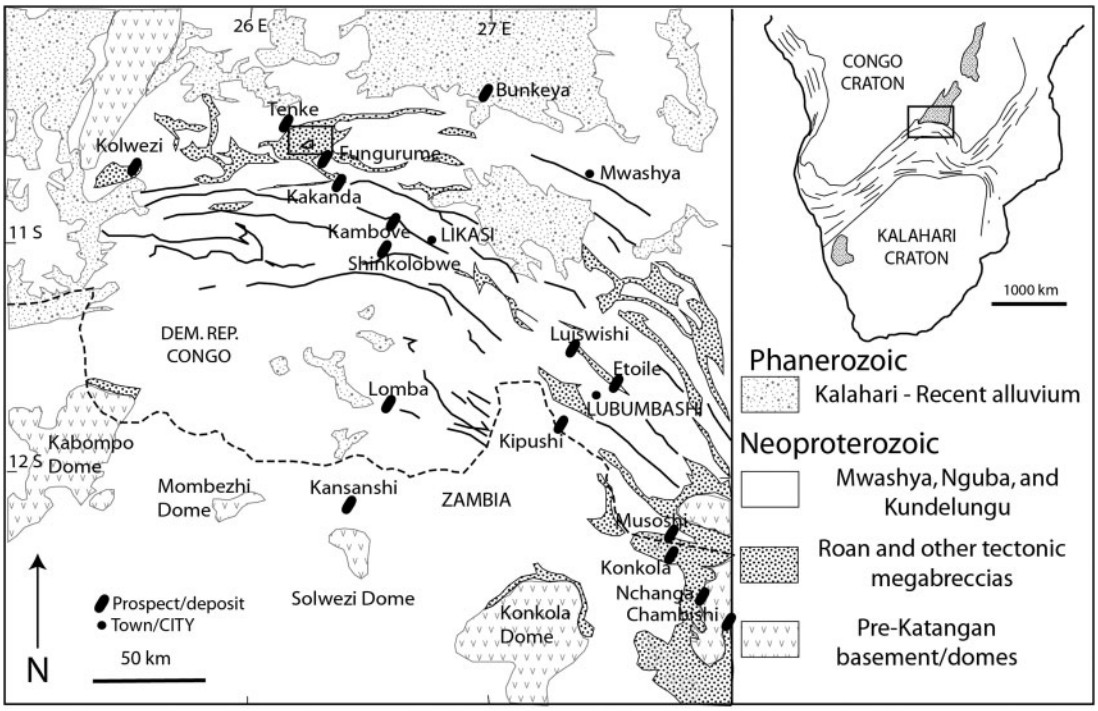

FIG. 1. Map of the Central African Copperbelt, showing the Tenke-Fungurume district.

during this period (Barra 2005). Some of the ore sulfides were remobilized into these veins, presumably as the orogeny proceeded (Selley *et al.* 2005).

After the orogeny, erosion exposed the Mines Series rocks to meteoric waters, which dissolved the sulfides and dolomite near the surface. Some of the metals from the sulfides combined with the carbonate from the dolomite to form malachite (Fig. 2). Chrysocolla, heterogenite, pseudomalachite, and rare cornetite, brochantite, and libethenite are also present among the supergene minerals nearest the surface (De Putter *et al.* 2010, Fay & Barton 2012). At greater depths, the supergene Cu minerals are native copper, chalcocite, and cuprite, and the supergene Co minerals are carbonates. These carbonate ores persist to great depths, in some places >750 m below the surface (Fay & Barton 2012).

Description

Cobalt-rich dolomite and calcite form euhedral crystals up to a few centimeters long, with either rhombic morphology or crest habits. Both carbonates also occur as fine disseminated crystals. Cobalt-rich dolomite is most common as Co-rich bands in otherwise normal dolomite, optically continuous with the rest of the dolomite crystal. Members of the spherocobaltite-magnesite solid solution $(Mg,Co)CO_3$ form elongate and prismatic crystals with hexagonal cross sections. At up to 1 mm in length, such crystals are the largest and the most noticeable occurrence of $(Mg,Co)CO_3$, which also occurs as inclusions <5 microns across. These inclusions typically consist of magnesian spherocobaltite and kolwezite (Fig. 3). These are common in supergene chalcocite and create the characteristic texture visible in Figure 3.

Their pink color distinguishes the Co-bearing from other rhombohedral carbonates (Fig. 3). In hand samples of cobaltoan carbonates, the color is intense even in specimens with less than 5 wt.% Co. In dolomites and calcites the pink tinge is much subtler in thin section, where all but the most Co-rich crystals are only pale pink in plane-polarized light and look no different from ordinary dolomites and calcites with the polars crossed. By contrast, spherocobaltite and compositions along the join towards magnesite retain their intense pink color in thin section. Even in cross-polarized light they have a rosy cast. This intensity of color, and the lack of effervescence even in powdered specimens, distinguishes members of the magnesite-spherocobaltite solid solution from the cobaltoan dolomites.

All the Co-carbonates are uniaxial, optically negative, and highly birefringent (maximum $\delta = 0.18$).

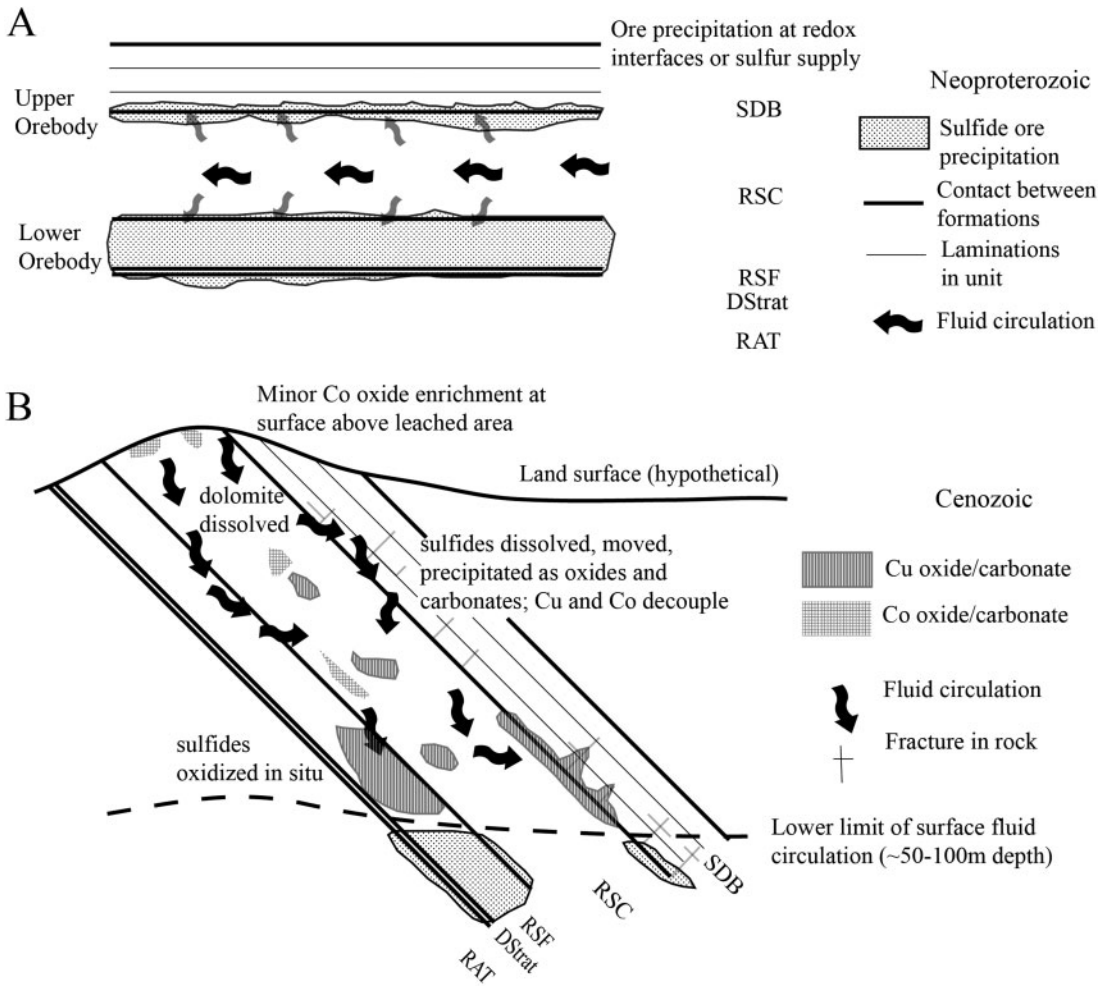

FIG. 2. Schematic cross sections showing processes of ore formation at Tenke-Fungurume: hypogene sulfide deposition during diagenesis (A) and supergene alteration of the sulfide ores to oxides and carbonates (B).

Their Mohs hardnesses are 3.5–4. The presence of Co, and in many cases of Fe, quenches the normally bright cathodoluminescence of a carbonate.

Occurrence patterns and abundance

Cobalt-rich carbonates are not stable at the surface over most of the Central African Copperbelt but are sometimes present on freshly dug surfaces at a depth of a few meters. The tops of Copperbelt deposits contain Co mostly as heterogenite. The lower depths of deposits contain Co entirely as carrollite. Although minor Co-carbonate concentrations persist some way into the shallow heterogenite and deep carrollite zones, the vast majority of Co-rich carbonate occurs in the middle depths between them. Cobalt carbonate occurrences do not correlate with stratigraphy or with type of gangue, and most of them may be associated with any of the sulfide or oxide ore minerals. The exception is the inclusion type of $(Mg,Co)CO_3$, which follows the distribution of the supergene chalcocite that hosts it.

Core loggers and most research geologists generally consider Co-rich dolomite the most abundant of the Co-carbonates in the Copperbelt by far. However, more than a dozen samples recorded as Co-rich dolomite during fieldwork and petrography have proven on reexamination to be Co-rich magnesite or Mg-rich spherocobaltite. Thus, it is likely that much of the pink carbonate recorded in core logs and maps as

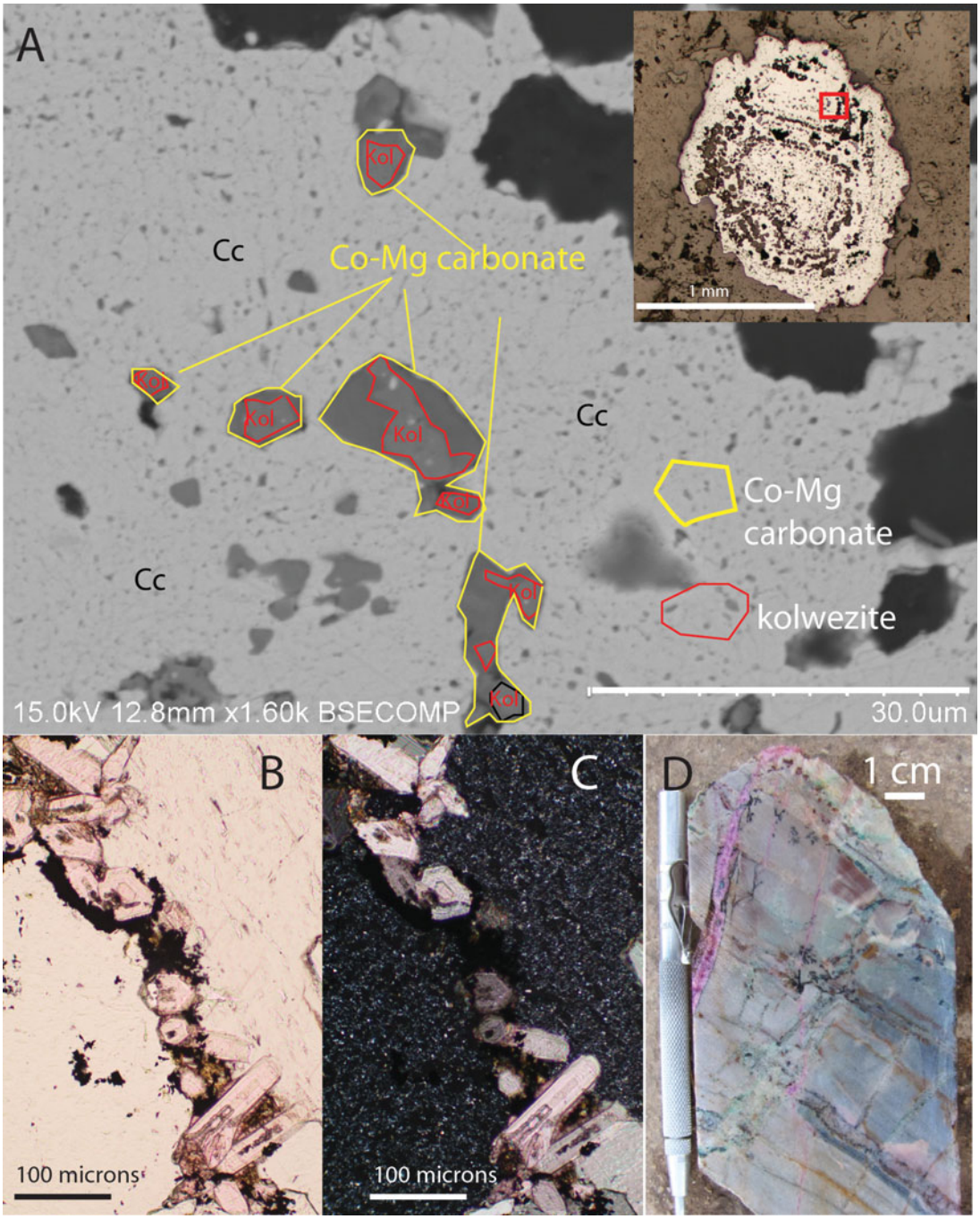

FIG. 3. Typical occurrence of Co-rich carbonates at TFM. (A) Kolwezite-cored inclusions of Mg-rich spherocobaltite in a chalcocite grain replacing carrollite, sample F23R-347.05; cc = chalcocite. (B) Crystalline variety of $(Mg,Co)CO_3$ in thin section, plane-polarized transmitted light, sample F65-113.5. (C) The same, in cross-polarized transmitted light. (D) Typical occurrence of Co-carbonate in hand sample F12-200.8.

Co-rich dolomite is in fact $(Mg,Co)CO_3$. This makes it impossible to judge which Co carbonates are most abundant, how abundant they are, and where each may be distributed, except for their collective restriction to the middle depths of ore deposits.

Textural relationships to other minerals

Cobalt carbonates overgrow or crosscut most of the other minerals in the Copperbelt host rocks and also occupy void spaces left by dissolution of preexisting minerals. Malachite, heterogenite, native copper, chrysocolla, pseudomalachite, brochantite, kolwezite, and libethenite are the only minerals not crosscut or overgrown by the Co-carbonates; they have the same textural relationships as the Co-carbonates and appear to have formed at the same time. This mineral association and textural relationships indicate that the Co-carbonates and other minerals crystallized late in the paragenesis of alteration, probably during supergene circulation.

Electron microprobe analyses of TFM Co-rich carbonates

Table 2 shows representative compositions of the Co-rich carbonates analyzed in this study using a Cameca SX100 electron probe microanalyzer (EPMA) at the University of Arizona. Table 3 summarizes the analytical conditions, and Table 4 gives the compositions of the standards used during analysis. The analytical results were normalized to a total of 7.0 atoms per formula unit for dolomites and to 5.0 *apfu* for magnesite-spherocobaltite.

These results show that the magnesite-spherocobaltite solid solution is complete even in the low-temperature supergene specimens in this study. The measured compositions range from $Co_{0.81}Mg_{0.15}CO_3$ (Table 2, sample F9-135.9jv) to $Mg_{0.75}Co_{0.24}CO_3$ (Table 2, sample cp-4) with Fe, Mn, and Ca making up the balance of the cation content. Much of this compositional range is present even in single crystals: backscatter imaging with a JEOL 6010LA SEM showed strong compositional zoning concentric around the *c*-axis of several crystals (Fig. 4). One of them varied from a core of $Mg_{0.49}Co_{0.48}CO_3$ to a rim of $Mg_{0.84}Co_{0.15}CO_3$ (Fig. 5).

Most of the Co-rich dolomite specimens analyzed in this study contain less than 2 mol.% Co (Table 2). This is typical for the Copperbelt (Simmonds 1980), although experimental data obtained at high temperature suggest that Co-rich dolomites may contain up to 20 mol.% Co (Goldsmith & Northrop 1965). Mineva-Stefanova (1997) reported a specimen from an unknown location with 35 mol.% Co. The analyses from TFM include no specimen with such high Co and only a few with significantly elevated Co: for

TABLE 2. REPRESENTATIVE CHEMICAL ANALYSES OF CARBONATE MINERALS FROM TENKE-FUNGURUME

Sample; mineral[1]	F65-113.5-1; mg-sp ss	F65-113.5-2; mg-sp ss	F65-113.5-4; mg-sp ss	F65-113.5-5; mg-sp ss	F65-113.5-6; mg-sp ss	F65-113.5-7; mg-sp ss	F137-239.5; dol	F140-540.9; dol
MgO (wt.%)	19.85	20.60	32.46	30.88	31.40	29.66	21.66	21.38
CaO	0.94	0.84	0.12	0.14	0.12	0.40	30.65	30.47
MnO	0.27	0.20	<0.05[#]	<0.05	<0.05	0.15	0.05	BDL
FeO	0.23	0.21	0.27	0.24	0.13	0.81	0.16	0.09
CoO	36.08	34.40	19.60	21.95	21.12	23.38	0.03	BDL
NiO	<0.02	<0.02	0.03	0.02	0.03	0.04	0.03	BDL
ZnO	0.06	0.09	<0.01	0.01	<0.01	0.09	0.04	BDL
SrO	<0.01	<0.01	<0.01	<0.01	<0.01	<0.01	0.02	BDL
CO_2*	43.94	43.66	47.25	46.92	46.91	47.09	47.90	47.34
total	101.37	100.00	99.73	100.17	99.71	101.61	100.53	99.27
Mg *apfu*	0.493	0.515	0.750	0.719	0.731	0.688	0.987	0.986
Ca	0.017	0.015	0.002	0.002	0.002	0.007	1.004	1.010
Mn	0.004	0.003	0.001	0.000	0.001	0.002	0.001	0.001
Fe	0.003	0.003	0.003	0.003	0.002	0.011	0.004	0.002
Co	0.482	0.463	0.244	0.275	0.264	0.292	0.001	0.000
Ni	0.000	0.000	0.000	0.000	0.000	0.000	0.001	0.000
Zn	0.001	0.001	0.000	0.000	0.000	0.001	0.001	0.000
Sr	0.000	0.000	0.000	0.000	0.000	0.000	0.000	0.000

TABLE 2 (CONTINUED). REPRESENTATIVE ANALYSES OF CARBONATE MINERALS FROM TENKE-FUNGURUME

Sample; mineral[1]	F177-53.9-1; dol	F177-53.9-2; dol	F177-53.9-3; dol	F178-75.9-1; dol	F178-75.9-2; dol	F178-75.9-3; dol	F184-65.9-1; dol	F184-65.9-2; dol
MgO (wt.%)	18.12	21.89	20.96	21.74	20.93	14.39	21.82	21.54
CaO	29.26	29.90	29.00	30.66	29.80	29.30	30.53	30.31
MnO	0.81	<0.05	0.16	<0.05	0.08	0.06	0.10	0.11
FeO	0.93	0.08	0.66	0.05	<0.05	<0.05	0.27	0.22
CoO	4.34	0.09	0.55	<0.02	1.74	11.41	<0.02	0.71
NiO	0.02	<0.02	BDL	<0.02	<0.02	<0.02	<0.02	<0.02
ZnO	0.02	<0.01	BDL	<0.01	0.03	0.02	<0.01	<0.01
SrO	0.06	0.02	0.90	0.02	<0.01	0.01	0.01	0.02
CO_2*	46.41	47.49	46.86	47.87	47.33	45.46	48.01	47.94
total	99.96	99.46	99.09	100.34	99.91	100.65	100.74	100.86
Mg *apfu*	0.853	1.007	0.977	0.992	0.966	0.691	0.992	0.981
Ca	0.989	0.988	0.971	1.005	0.988	1.012	0.998	0.992
Mn	0.022	0.001	0.004	0.001	0.002	0.002	0.002	0.003
Fe	0.025	0.002	0.017	0.001	0.000	0.000	0.007	0.006
Co	0.110	0.002	0.014	0.000	0.043	0.295	0.000	0.017
Ni	0.000	0.000	0.000	0.000	0.000	0.000	0.000	0.000
Zn	0.001	0.000	0.000	0.000	0.001	0.000	0.000	0.000
Sr	0.001	0.000	0.016	0.000	0.000	0.000	0.000	0.000

TABLE 2 (CONTINUED). REPRESENTATIVE ANALYSES OF CARBONATE MINERALS FROM TENKE-FUNGURUME

Sample; mineral[1]	F192-53.2; dol	F264-167.3B; dol	F264-176.3; dol	F41-66.8; dol	F62R-2854; dol	F65-113.5-8; dol	F65-113.5-9; dol	F65-113.5-10; mg-sp ss
MgO (wt.%)	21.47	21.45	21.58	21.82	19.75	20.22	21.74	19.72
CaO	30.51	30.35	30.47	30.34	30.02	29.87	30.60	0.91
MnO	0.27	0.12	0.08	0.08	0.90	0.47	<0.05	0.24
FeO	0.57	0.63	0.24	0.06	2.47	0.67	0.07	0.21
CoO	<0.02	<0.02	<0.02	0.03	<0.02	1.78	<0.02	36.05
NiO	<0.02	<0.02	<0.02	<0.02	0.01	<0.02	<0.02	<0.02
ZnO	0.04	0.02	0.01	<0.01	0.05	<0.01	<0.01	0.07
SrO	0.02	0.02	0.02	0.02	0.02	<0.01	<0.01	<0.01
CO_2*	47.93	47.72	47.69	47.76	47.24	47.27	47.82	43.74
total	100.79	100.32	100.09	100.13	100.46	100.28	100.23	100.95
Mg *apfu*	0.978	0.982	0.988	0.998	0.913	0.934	0.993	0.492
Ca	0.999	0.998	1.003	0.997	0.997	0.992	1.004	0.016
Mn	0.007	0.003	0.002	0.002	0.024	0.012	0.001	0.003
Fe	0.015	0.016	0.006	0.002	0.064	0.017	0.002	0.003
Co	0.000	0.000	0.000	0.001	0.000	0.044	0.000	0.484
Ni	0.000	0.000	0.000	0.000	0.000	0.000	0.000	0.000
Zn	0.001	0.000	0.000	0.000	0.001	0.000	0.000	0.001
Sr	0.000	0.000	0.000	0.000	0.000	0.000	0.000	0.000

example, $Ca_{1.01}(Mg_{0.69}Co_{0.29})(CO_3)_2$ (Table 2, sample F178-75.9) and $Ca_{1.02}(Mg_{0.76}Co_{0.21})(CO_3)_2$ (Table 2, sample Kw364-218.4B).

No data exist on the composition of kolwezite in the Copperbelt, and the only specimens available at TFM were the kolwezite-magnesian spherocobaltite inclusions, in which the kolwezite proved too small to analyze. No kolwezite amid the inclusions measured more than 10 microns long, and most of them were less than 3 microns in length.

TABLE 2 (CONTINUED). REPRESENTATIVE ANALYSES OF CARBONATE MINERALS FROM TENKE-FUNGURUME

Sample; mineral[1]	F65-113.5-11; mg-sp ss	F65-60.8; dol	F9-114.3; dol	F9-135.9jv; mg-sp ss	Fw82-139.8; dol	Fw82-145A; dol	K2365-125.3; dol	Kf284-524; mg
MgO (wt.%)	16.66	21.49	21.56	5.14	21.65	21.46	20.56	48.07
CaO	0.85	30.19	30.25	0.55	30.23	30.32	30.68	0.04
MnO	0.20	0.13	0.11	0.10	0.14	0.09	0.13	0.10
FeO	0.30	0.63	0.32	1.66	0.46	0.49	0.59	0.14
CoO	39.61	<0.02	<0.02	53.09	<0.02	<0.02	0.02	<0.02
NiO	<0.02	<0.02	<0.02	0.63	<0.02	<0.02	0.02	<0.02
ZnO	0.02	0.10	<0.01	0.01	<0.01	<0.01	0.04	<0.01
SrO	<0.01	0.04	<0.01	BDL	0.01	0.02	0.03	<0.01
CO_2*	42.44	47.68	47.56	38.68	47.74	47.60	47.03	52.66
total	100.08	100.24	99.80	99.86	100.23	99.97	99.11	101.01
Mg *apfu*	0.429	0.984	0.990	0.145	0.990	0.985	0.955	0.997
Ca	0.016	0.994	0.998	0.011	0.994	1.000	1.024	0.001
Mn	0.003	0.003	0.003	0.002	0.004	0.002	0.004	0.001
Fe	0.004	0.016	0.008	0.026	0.012	0.013	0.015	0.002
Co	0.548	0.000	0.000	0.806	0.000	0.000	0.001	0.000
Ni	0.000	0.000	0.000	0.010	0.000	0.000	0.001	0.000
Zn	0.000	0.002	0.000	0.000	0.000	0.000	0.001	0.000
Sr	0.000	0.001	0.000	0.000	0.000	0.000	0.000	0.000

TABLE 2 (CONTINUED). REPRESENTATIVE ANALYSES OF CARBONATE MINERALS FROM TENKE-FUNGURUME

Sample; mineral[1]	Kw300-1584B; dol	Kw364-218.4B-1; dol	Kw364-218.4B-2; dol	Kw365-154.3A; dol	MgCo2 core; mg-sp ss	MgCo2 mid; mg-sp ss	MgCo2 rim; mg-sp ss	T158-159.8B; dol
MgO (wt.%)	21.69	21.65	15.91	21.40	32.66	32.04	28.74	21.75
CaO	30.17	29.95	29.80	30.49	0.63	0.09	0.44	30.33
MnO	0.15	0.19	0.05	0.10	0.17	<0.05	<0.05	0.17
FeO	0.52	0.51	0.10	0.40	0.22	0.28	0.12	0.36
CoO	0.02	<0.02	8.10	BDL	19.81	20.02	25.25	<0.02
NiO	<0.02	<0.02	<0.02	BDL	<0.02	0.02	0.04	<0.02
ZnO	0.03	0.10	<0.01	0.03	0.08	<0.01	0.01	0.02
SrO	0.01	0.04	<0.01	0.01	<0.01	<0.01	<0.01	0.03
CO_2*	47.81	47.65	45.62	47.63	48.08	47.03	46.68	47.90
total	100.40	100.08	99.59	100.06	101.64	99.48	101.28	100.56
Mg *apfu*	0.991	0.992	0.762	0.981	0.742	0.744	0.672	0.991
Ca	0.990	0.986	1.025	1.005	0.010	0.002	0.007	0.994
Mn	0.004	0.005	0.001	0.003	0.002	0.001	0.000	0.004
Fe	0.013	0.013	0.003	0.010	0.003	0.004	0.002	0.009
Co	0.001	0.000	0.209	0.000	0.242	0.250	0.318	0.000
Ni	0.000	0.000	0.000	0.000	0.000	0.000	0.000	0.000
Zn	0.001	0.002	0.000	0.001	0.001	0.000	0.000	0.000
Sr	0.000	0.001	0.000	0.000	0.000	0.000	0.000	0.001

[1]Mineral abbreviations: mg-sp ss = magnesite-spherocobaltite solid solution; dol = dolomite; mg = magnesite.
*CO_2 calculated from stoichiometry.
*"<"values for the oxides are based on and calculated from 3σ elemental detection limits: Ca 250 ppm; Mn 349 ppm; Fe 348 ppm; Co 134 ppm; Ni 100 ppm; Zn 74 ppm; and Sr 78 ppm. A few Mn *apfu* values ostensibly below detection limit appear as 0.001 due to rounding errors.

TABLE 3. ANALYTICAL CONDITIONS FOR ELECTRON PROBE MICROANALYZER ANALYSES, CAMECA SX100

Element	Beam current (nA)	Dwell time (s)	Voltage (keV)	Detector	Avg. det. Limit (ppm)
Mg	10	20	20	TAP	459
Ca	10	20	20	LPET	250
Fe	10	20	20	LLIF	348
Mn	10	20	20	LLIF	349
Co	100	60	20	TAP	134
Ni	100	60	20	LPET	100
Zn	100	60	20	LLIF	74
Sr	100	60	20	LLIF	78

Cobalt-rich calcite was not detected in any TFM sample.

X-ray diffraction and Raman spectrum of (Mg,Co)CO_3

An 80 μm-long crystal of Co-rich magnesite ($Mg_{0.63}Co_{0.37}CO_3$ based on SEM-EDS analysis) was examined with single-crystal X-ray diffraction using a Bruker X8 APEX2 CCD X-ray diffractometer equipped with graphite-monochromatized MoK radiation. This yielded unit cell parameters $a = b =$ 4.6537(4), c = 15.003(1)Å, and V = 281.38(4) Å^3. This unit cell volume is 1.58 Å^3 larger than the corresponding weighted average of 63% of the $MgCO_3$ (279.05 Å^3) and 37% of the $CoCO_3$ (281.07 Å^3) unit cells, which was calculated as 279.80 Å^3. However, this volume difference is probably not large enough to destabilize the (Mg,Co)CO_3 solid solution at high pressures. The structure determination demonstrates that this Co-magnesite possesses the calcite-type structure (space group R-3c).

The Raman spectrum of the same Co-rich magnesite crystal was then collected in a random orientation with a Thermo Almega microRaman system using a 532 nm solid-state laser with a thermoelectric-cooled CCD detector. The laser is partially polarized with 4 cm^{-1} resolution and a spot size of 1 μm. Comparison with the Raman spectra for magnesite (R050443) and spherocobaltite (R060497) in the RRUFF database (http://rruff.info) reveals that the Raman bands obtained from the Co-magnesite crystal lie intermediate between magnesite and spherocobaltite and have no extraneous peaks (Fig. 6). Similar results have been observed for the magnesite-siderite solid solutions (Boulard *et al.* 2012), indicating that Co affects the structures of calcite-type carbonates in a way similar to Fe and other transition metals in carbonate solid solution.

Discussion

Inferred Mg–Ca–Co carbonate phase relations at low T

The only existing chemical data for the $MgCO_3$–$CoCO_3$ system are from samples synthesized at 600–800 °C and 15–25 kbar and these indicate complete solid solution (Goldsmith & Northrop 1965). The Raman spectrum, X-ray diffraction data, and chemical compositions in this study (Fig. 7) show that a complete solid solution between magnesite and spherocobaltite persists to the pressure-temperature conditions of the supergene environment—probably near-surface pressure and temperature < 50 °C. Figure 8 shows the inferred phase relations among Mg, Co, and Ca carbonates in this pressure-temperature regime. The maximum possible concentration of Co in dolomite is uncertain, but the present study analyzed dolomites with as much as 8.9 mol.% Co (11.41% CoO; Table 2, sample F178-75.9). Goldsmith & Northrop (1965) calculated a theoretical limit of 20% Co.

TABLE 4. COMPOSITIONS OF ELECTRON MICROPROBE STANDARDS USED IN ANALYSES (wt.%)

Element/ Standard	Mg / $MgCO_3$	Ca / $CaCO_3$	Fe / $FeCO_3$	Mn / $MnCO_3$	Si	Al	Ni / Ni-diopside	Co / Co-diopside	Zn / ZnO	Sr / $SrCO_3$	C	O
Mg	28.44	0.04	0.68	0.02							14.19	56.74
Ca		40.09									12.01	48
Fe			45.92	2.28							10.34	41.36
Mn	0.57	0.02	0.17	46.66							10.51	42.02
Co	10.49	16.8			24.68			4.91				43.06
Ni	8.62	17.87	0.12		24.91	0.45	5.06					43.01
Zn				1.13					79.45			19.77
Sr		1.36								57.22	8.25	32.97

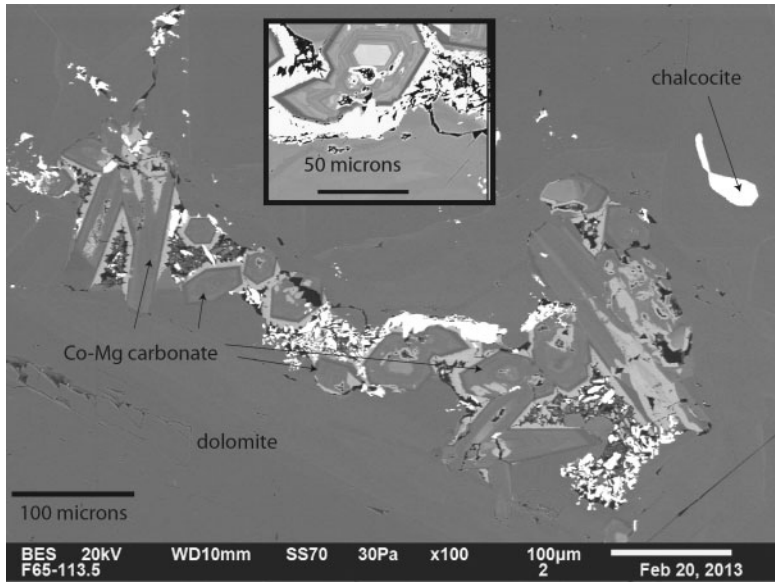

FIG. 4. Crystalline variety of magnesite-spherocobaltite solid solution, in backscatter, showing zoning within crystals. Sample F65-113.5, BSE image of Figure 3B-3C.

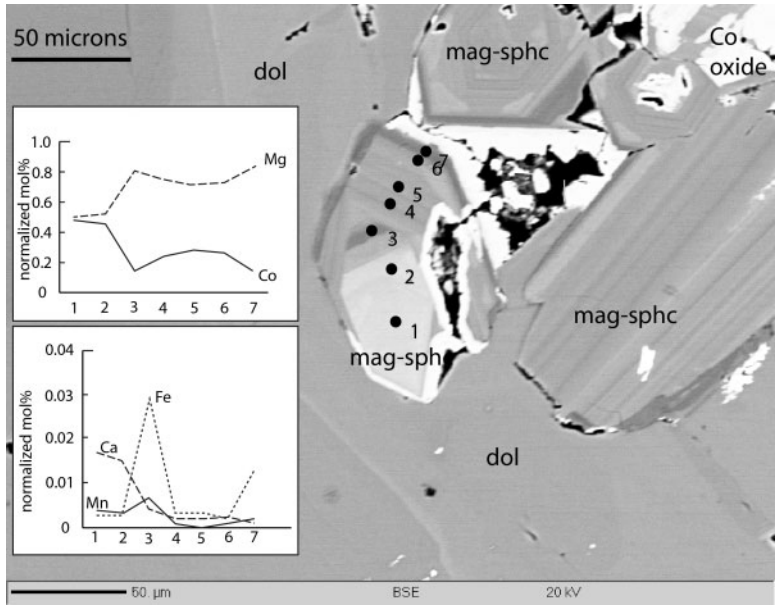

FIG. 5. Comparison of backscatter image of Co-rich magnesite (mag-sphc) with compositions determined by EPMA at marked points 1–7. Sample F65-113.5-1 through F65-113.5-7 in Table 2; F65-113.5-3 was excluded from the Table due to a poor total.

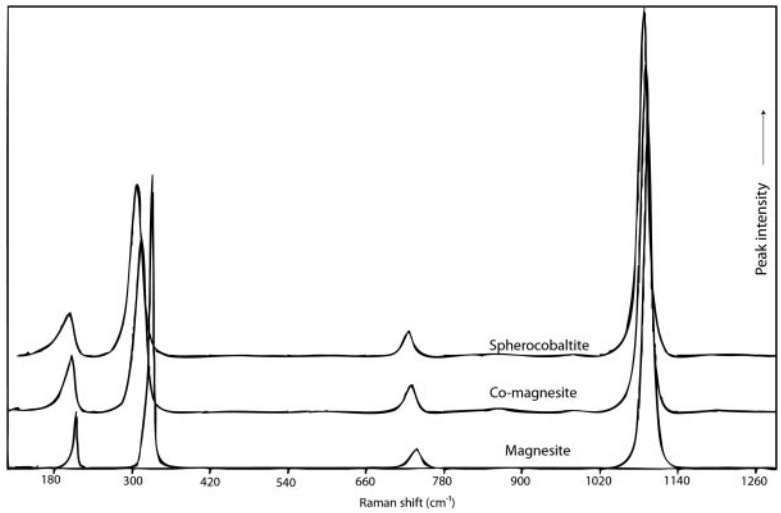

FIG. 6. Raman spectra of spherocobaltite, magnesite, and a member of the magnesite-spherocobaltite solid solution.

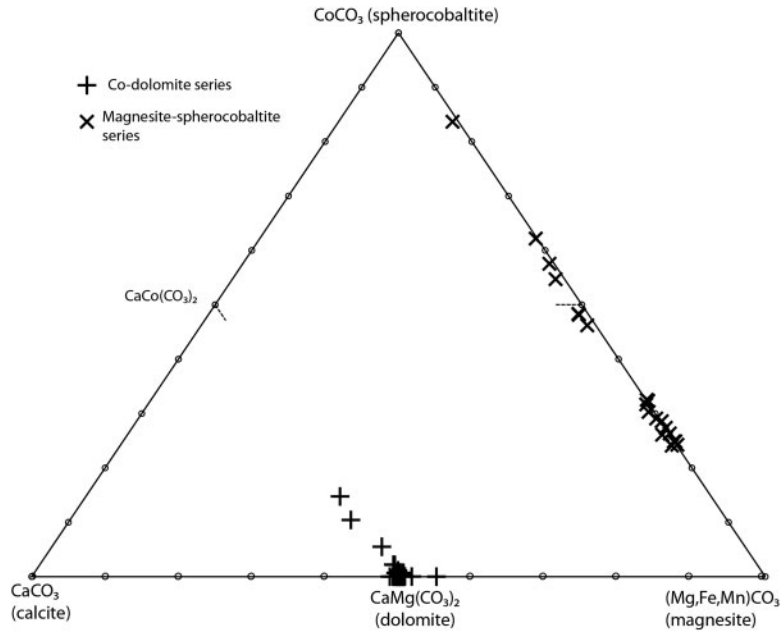

FIG. 7. Ca–Co–Mg-carbonate ternary diagram showing compositions of species analyzed in this study.

Formation of Co-bearing carbonates

The textural evidence cited above renders it virtually certain that the Co-carbonates at TFM formed in the supergene environment as circulating meteoric fluids dissolved dolomite and oxidized the sulfide ores, releasing metal ions. Some of the liberated Co was oxidized Co^{3+}, which formed heterogenite; some of the Co remained divalent and bonded with the carbonate in the fluid, precipitating dolomite, Co-rich dolomite, Co-rich magnesite, and magnesian spherocobaltite. The following section

will focus on the potential precipitation mechanisms of each of these in turn.

Dolomite precipitation at low temperature is a vexed issue in the geochemical and geological literature (*e.g.*, Baker & Kastner 1981, Land 1998, Warren 2000), and most explanations of low-temperature dolomite formation involve dolomitization of a preexisting calcite during diagenesis of sedimentary rock (*e.g.*, Hardie 1987). However, this is not a viable mechanism for producing the supergene Co-rich dolomite as observed at TFM. Cobalt would be evenly distributed through dolomite crystals produced by dolomitization of a calcite, whereas in the TFM samples, Co-rich dolomite occurs as high-Co bands in normal Ca-Mg dolomites. Primary precipitation of a variably Co-rich dolomite offers the best explanation for this banded character, even though primary precipitation of dolomite remains problematic from a kinetic standpoint (Lovering 1969). Under this hypothesis, the high-Co bands represent transient episodes of Co enrichment in the dolomite-precipitating fluid, probably a result of dissolution of nearby carrollite. Such a fluid must also have been considerably enriched in Mg relative to Ca, as dolomite cannot precipitate from a fluid with Mg/Ca < 5.2 (Warren 2000). The possible mechanisms for supergene origin of such an Mg-enriched fluid are enigmatic.

Potential formation mechanisms of the magnesian spherocobaltites are even less clear. Boni *et al.* (2011) have textural evidence that Mg-rich smithsonite in the Jabali deposit (Yemen), analogous to the Mg-rich spherocobaltites at TFM, formed by dedolomitization of a Zr-rich dolomite. Dedolomitization is a common geological phenomenon, especially in the supergene environment (Dockal 1988). It consists of ion exchange:

$$CaMg(CO_3)_2 + Ca^{2+} = 2CaCO_3 + Mg^{2+} \quad (1)$$

or

$$CaMg(CO_3)_2 + Mg^{2+} = 2MgCO_3 + Ca^{2+} \quad (2)$$

Dedolomitization by Equation (1) occurs at low $a\mathrm{Mg}^{2+}/a\mathrm{Ca}^{2+}$ (Rosenberg *et al.* 1967) and produces calcite plus an Mg-enriched fluid. Dedolomitization by Equation (2) is less common and, for a pure Ca-Mg dolomite, produces magnesite plus a Ca-enriched fluid. If, however, the dolomite contains appreciable transition metals at the Mg site, dedolomitization by Equation (2) generates magnesite solid solutions rather than end-member magnesite (Boni *et al.* 2011). Thus, analogy with the Zn-carbonate system would suggest that $(Mg,Co)CO_3$ can form by dedolomitization of a cobaltoan dolomite:

$$10Ca(Mg_{0.9}Co_{0.1})(CO_3)_2 + 5Co^{2+} + 5Mg^{2+} = 10Ca^{2+} + 20Mg_{0.7}Co_{0.3}CO_3 \quad (3)$$

The added Co and Mg might come from dissolving nearby carrollite and dolomite. Significantly, Equation (3) demonstrates that adding equal proportions of Co and Mg results in Co enrichment in the magnesite relative to the parent Co-rich dolomite. The composition of the magnesite produced by Equation (3) is similar to the composition of many or most of the cobaltoan magnesites observed at TFM (Table 2).

From a geochemical point of view, Equation (3) offers a plausible explanation for the formation of the magnesite-spherocobaltite solid solution at TFM. However, the textural evidence contradicts it: the $(Mg,Co)CO_3$ crystals at TFM occur on dolomite grains that show no evidence of dissolution (Fig. 4). Still, dedolomitization might have been very localized, or might have occurred elsewhere and the components transported to the site of supergene magnesite-spherocobaltite. Figure 8 shows a possible pathway for fluid and crystal following dedolomitization of a cobaltoan dolomite.

The kolwezite-$(Mg,Co)CO_3$ inclusions common in supergene chalcocite are more likely to have formed by direct precipitation from pockets of Mg-Cu-Co-carbonate fluid trapped within the chalcocite grain as it replaced carrollite. The observation that kolwezite is invariably at the centers of the inclusions and $(Mg,Co)CO_3$ is invariably at the edges suggests that $(Mg,Co)CO_3$ precipitated first. Crystallization of magnesian spherocobaltite proceeded either until Mg was exhausted or until Cu reached saturation in the remaining fluid, which then crystallized kolwezite (Fig.3). A possible reaction is:

$$CaMg(CO_3)_2 + CuCo_2S_4 + 4H_2O + CO_2 + 7.5O_2 = 3H_2SO_4 + CuCo(CO_3)(OH)_2 + 2(Mg,Co)CO_3 + CaSO_{4(aq)} \quad (4)$$

Equation (4) is balanced for $Mg_{0.5}Co_{0.5}CO_3$, although the compositions of the inclusions are typically closer to spherocobaltite. An equation for end-member spherocobaltite might be:

$$3CuCo_2S_4 + 6CO_2 + 12H_2O + 2O_2 = CuCo(CO_3)(OH)_2 + 5CoCO_3 + Cu_2S + 11H_2SO_4 \quad (5)$$

Equations (3)–(5) are all potentially viable methods for producing magnesite-spherocobaltite solid solution in the supergene environment, although there are objections to Equation (3) based on the textural evidence cited above. Any or all of the processes represented by these equations may have contributed to forming magnesite-spherocobaltite solid solution at

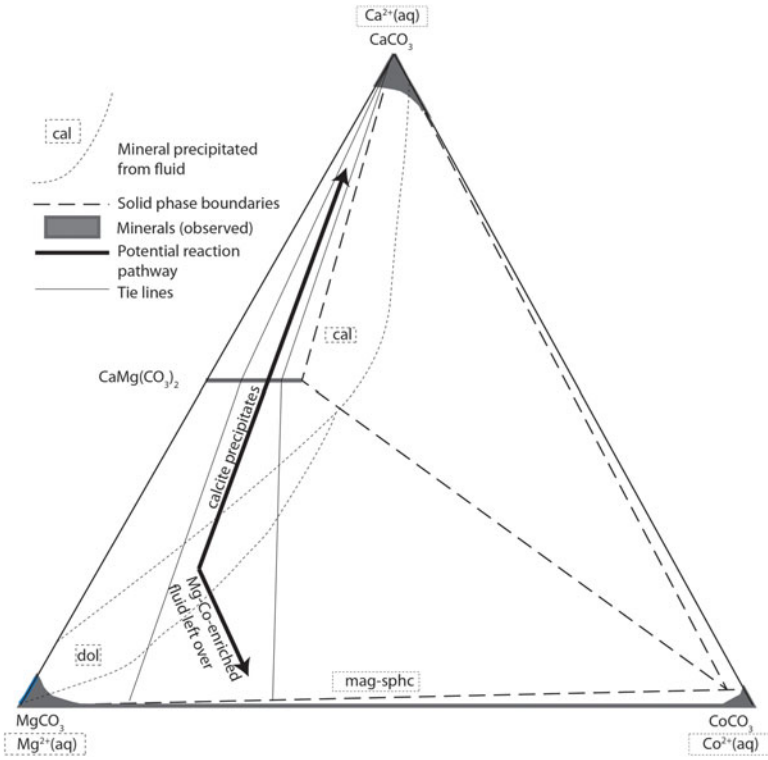

FIG. 8. Ternary diagram showing the inferred phase relations among Ca-Mg-Co carbonates at supergene pressure-temperature conditions, the minerals stable in fluids of different compositions, and one potential way to form magnesite-spherocobaltite solid solution by dedolomitization of a Co-rich dolomite.

TFM, and the present evidence is not enough to judge their relative roles.

Although they are best known from the supergene zones of Central African Copperbelt deposits, Co-rich carbonates can form in the hypogene environment. A specimen from Bou Azzer (Morocco) contains Co-rich dolomite intergrown with primary skutterudite ($CoAs_3$). This indicates that Co carbonates can precipitate under hypogene conditions. Hypogene Co-carbonate precipitation is probably limited to systems that are deficient in As and S relative to Co and CO_3; otherwise, Co sulfides, arsenides, and arsenates precipitate. This is consistent with the finding of Markl *et al.* (2014) that spherocobaltite and cobaltoan calcite are unstable with respect to erythrite ($Co_3AsO_4{\cdot}8H_2O$) if even the tiniest amount of As is present in solution.

Solubility and metallurgical implications

The solubilities of rhombohedral carbonates are highly variable (Railsback 1999). Solubility calculations for dolomite, calcite, magnesite, and spherocobaltite show that spherocobaltite is insoluble compared to the Ca and Mg carbonates. Furthermore, in members of carbonate solid solutions such as $(Mg,Co)CO_3$, the cations present are not all liberated at the same rate when the mineral begins to dissolve; some cations enter solution more readily than the others. Solubility calculations for dolomite, magnesite, calcite, and spherocobaltite show that in all of them, Ca^{2+} and Mg^{2+} enter solution more readily than Co^{2+}; the difference is three to four orders of magnitude (Fig. 9). Any acid added to a mixed Ca-Co or Mg-Co carbonate will liberate all the available Ca or Mg before it liberates almost any of the Co. This is unfortunate from a metallurgical standpoint: it means that processing acid will dissolve every Ca-Mg carbonate in the vicinity and every other major cation in the Ca-Co or Mg-Co carbonate before it liberates appreciable Co.

Cobalt recoveries from carbonate ores in the Copperbelt are predicted with the assumption that the ore is Co-rich dolomite. As detailed above, reexamination of supposed Co-rich dolomite samples from TFM demonstrated that many of them are $(Mg,Co)CO_3$. It is reasonable to think that members of

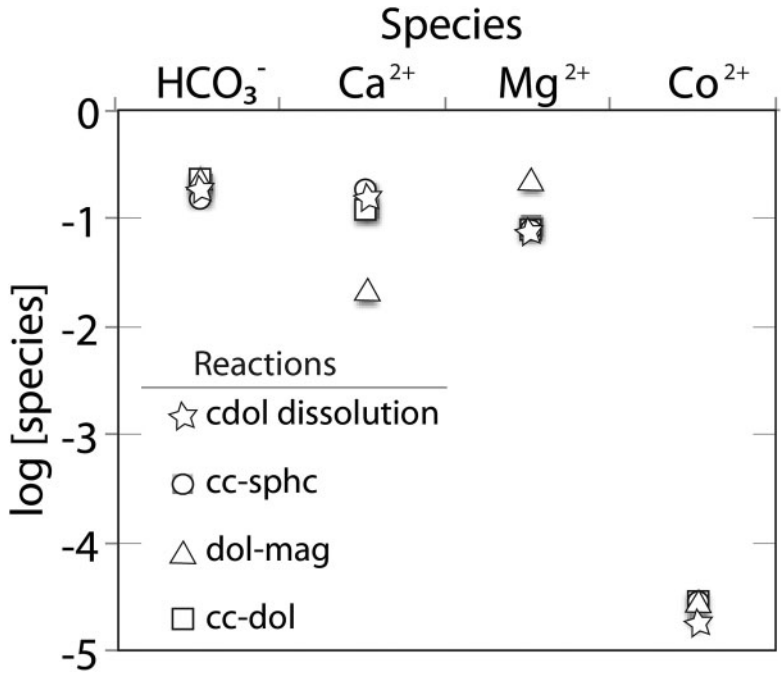

FIG. 9. Graph showing the log of the concentrations of the ions produced in reactions among the various carbonates. Cobalt is by far the least soluble ion in every reaction involving it. Calculated based on log K values from Robie & Hemingway (1995). cc = calcite, cdol = cobaltoan dolomite, dol = dolomite, mag = magnesite, sphc = spherocobaltite.

the magnesite-spherocobaltite solid solution may be present at other Copperbelt deposits and may have been recorded as Co-rich dolomite there, too. Inasmuch as Co in Mg-rich spherocobaltite is less amenable to acid leaching than Co in Co-rich dolomite, such misidentification could cause Co recoveries from Copperbelt ores to be significantly lower than predicted. Without more data on the occurrence and abundance of magnesite-spherocobaltite solid solution, however, it is impossible to say whether this represents a major cause of low recovery. Additional and regional-scale work on the distribution and abundance of the various Co carbonate species is needed.

CONCLUSIONS

Several carbonates of the calcite and dolomite groups contain appreciable Co: Co-rich dolomite, Co-rich calcite, spherocobaltite, and the solid solution of spherocobaltite and magnesite-spherocobaltite. Though they can form under hypogene conditions, Co-rich carbonates are more common in the supergene zones of Co ore deposits, where Cu-Co sulfides oxidize. In some cases, Co-rich dolomite and magnesian spherocobaltite are almost surely the products of primary precipitation; however, dedolomitization of Co-dolomite is another potential mechanism for creating $(Mg,Co)CO_3$. Solubility calculations suggest that Co carbonate ores will release all their contained Ca, Mg, and Fe ions before any significant Co when processed by acid leaching.

ACKNOWLEDGMENTS

The authors appreciate helpful reviews by Stan Evans, Eric Seedorff, Frank Mazdab, Frédéric Hatert, Simon Philippo, and an anonymous reviewer. Frank Mazdab also helped with the microprobe work and mineral normalizations. Research is supported by Freeport-McMoRan Copper & Gold and its affiliate Tenke-Fungurume Mine.

REFERENCES

ANOVITZ, L.M. & ESSENE, E.J. (1987) Phase equilibria in the system $CaCO_3$–$MgCO_3$–$FeCO_3$. *Journal of Petrology* **28**, 389–414.

BAKER, P.A. & KASTNER, M. (1981) Constraints on the formation of sedimentary dolomite. *Science* **213**, 214–216.

BARRA, F. (2005) Multi-stage and long-lived mineralization in the Zambian Copperbelt: Evidence from Re-Os geochronology. *In* Applications of the Re-Os Isotopic System in the Study of Mineral Deposits: Geochronology and Source of Metals. Unpublished Ph.D. thesis, University of Arizona, 211p.

BONI, M., MONDILLO, N., & BALASSONE, G. (2011) Zincian dolomite: A peculiar dedolomitization case? *Geology* **39**, 183–186.

BOULARD, E., GUYOT, F., & FIQUET, G. (2012) The influence on Fe content on Raman spectra and unit cell parameters of magnesite-siderite solid solutions. *Physics and Chemistry of Minerals* **39**, 239–246.

BROMILEY, F.A., BOFFA BALLARAN, T., LANGENHORST, F., & SEIFERT, F. (2007) Order and miscibility in the otavite-magnesite solid solution. *American Mineralogist* **92**, 829–836.

CAILTEUX, J. (1994) Lithostratigraphy of the Neoproterozoic Shaba-type (Zaire) Roan Supergroup and metallogenesis of the associated stratiform mineralization. *Journal of African Earth Sciences* **19**, 279–301.

CLISSOLD, M.E., LEVERETT, P., & WILLIAMS, P.A. (2003) Gaspéite-magnesite solid solutions and their significance. *In* Advances in Regolith (I.C. Roach, ed.). University of Western Sydney, Penrith South DC NSW, Australia (78–79).

DALTRY, V.D.C. (1991) African type-mineralogy: a general review (1838–1988). *Journal of African Earth Sciences* **13**, 313–322.

DALTRY, V.D.C. (1992) The type mineralogy of Africa: Zaire. Annales *de la* Société géologique *de* Belgique **115**, 33–62.

DE PUTTER, T., MEES, F., DECREE, S., & DEWAELE, S. (2010) Malachite, an indicator of major Pliocene Cu remobilization in a karstic environment (Katanga, Democratic Republic of Congo). *Ore Geology Reviews* **38**, 90–100.

DOCKAL, J. (1988) Thermodynamic and kinetic description of dolomitization of calcite and calcitization of dolomite (dedolomitization). *Carbonates and Evaporites* **3**, 125–141.

FAY, I. & BARTON, M. (2012) Alteration and ore distribution in the Proterozoic Mines Series, Tenke-Fungurume Cu–Co district, Democratic Republic of Congo. *Mineralium Deposita* **47**, 501–519.

FROST, R.L., WAIN, D.L., MARTENS, W.N., & REDDY, B.J. (2007) The molecular structure of selected minerals of the rosasite group – An XRD, SEM and infrared spectroscopy study. *Polyhedron* **26**, 275–283.

GAUTHIER, G. & DELIENS, M. (1999) Cobalt minerals of the Katanga Crescent, Congo. *Mineralogical Record* **30**, 255–267.

GOLDSMITH, J.R. & GRAF, D.L. (1960) Subsolidus relations in the system $CaCO_3$–$MgCO_3$–$MnCO_3$. *Journal of Geology* **68**, 324–335.

GOLDSMITH, J.R. & NORTHROP, D.A. (1965) Subsolidus phase relations in the systems $CaCO_3$–$MgCO_3$–$CoCO_3$ and $CaCO_3$–$MgCO_3$–$NiCO_3$. *Journal of Geology* **73**, 817–829.

HARDIE, L.A. (1987) Dolomitization: a critical view of some current views. *Journal of Sedimentary Research* **57**, 166–183.

HURLBUT, C.S. (1957) Zincian and plumbian dolomite from Tsumeb, South-West Africa. *American Mineralogist* **42**, 798–803.

KATSIKOPOULOS, D., FERNANDEZ-GONZALEZ, A., CARMELO PRIETO, A., & PRIETO, M. (2008) Co-crystallization of Co (II) with calcite: Implications for the mobility of cobalt in aqueous environments. *Chemical Geology* **254**, 87–100.

LAND, L.S. (1998) Failure to precipitate dolomite at 25° C from dilute solution despite 1000-fold oversaturation after 32 years. *Aquatic Geochemistry* **4**, 361–368.

LOVERING, T.S. (1969) The origin of hydrothermal and low temperature dolomite. *Economic Geology* **64**, 743–754.

MACKENZIE, F.T., BISCHOFF, W.D., BISHOP, F.C., LOIJENS, M., SCHOONMAKER, J., & WOLLAST, R. (1983) Magnesian calcites: Low-temperature occurrence, solubility and solid-solution behavior. *In* Carbonates: Mineralogy and Chemistry (R.J. Reeder, ed.). *Reviews in Mineralogy and Geochemistry* **11**, 97–144.

MARKL, G., MARKS, M., DERREY, I., & GUEHRING, J.-E. (2014) Weathering of cobalt arsenides: Natural assemblages and calculated stability relations among secondary Ca–Mg–Co arsenates and carbonates. *American Mineralogist* **99**, 44–56.

MINCEVA-STEFANOVA, J. (1997) First finding of high miscibility in the system $CaMg(CO_3)_2$–$CaCo(CO_3)_2$ in nature. *Geokhimiya, Mineralogiya i Petrologiya* **32**, 5–16.

NAVROTSKY, A. & LOUCKS, D. (1977) Calculation of subsolidus phase relations in carbonates and pyroxenes. *Physics and Chemistry of Minerals* **1**, 109–127.

OOSTERBOSCH, R. (1951) Copper mineralization in the Fungurume region, Katanga. *Economic Geology* **46**, 121–148.

PERCHIAZZI, N. & MERLINO, S. (2006) The malachite-rosasite group: crystal structures of glaukosphaerite and pokrovskite. *European Journal of Mineralogy* **18**, 787–792.

PIRARD, C. & HATERT, F. (2008) The sulfides and selenides of the Musonoi mine, Kolwezi, Katanga, Democratic Republic of Congo. *Canadian Mineralogist* **46**, 219–231.

RAILSBACK, L.B. (1999) Patterns in the compositions, properties, and geochemistry of carbonate minerals. *Carbonates and Evaporites* **14**, 1–20.

REEDER, R.J. (1983) Crystal chemistry of the rhombohedral carbonates. *In* Carbonates: Mineralogy and Chemistry (R.J. Reeder, ed.). *Reviews in Mineralogy and Geochemistry* **11**, 1–47.

REEDER, R.J., LAMBLE, G.M., & NORTHRUP, P.A. (1999) XAFS study of the coordination and local relaxation around Co^{2+}, Zn^{2+}, Pb^{2+}, and Ba^{2+} trace elements in calcite. *American Mineralogist* **84**, 1049–1060.

ROBIE, R.A. & HEMINGWAY, B.S. (1995) Thermodynamic properties of minerals and related substances at 298.15 K and 1 bar (10^5 Pascals) pressure and at higher temperatures. *Bulletin of the U.S. Geological Survey* **2131**, 461p.

ROSENBERG, P.E. & FOIT, F.F. (1979) The stability of transition metal dolomites in carbonate systems: a discussion. *Geochimica Cosmochimica Acta* **43**, 951–955.

ROSENBERG, P.E., BURT, D.M., & HOLLAND, H.D. (1967) Calcite-dolomite-magnesite stability relations in solutions: the effect of ionic strength. *Geochimica Cosmochimica Acta* **31**, 391–396.

SCHUH, W., LEVEILLE, R., FAY, I., & NORTH, R. (2012) Geology of the Tenke-Fungurume sediment-hosted stratabound copper-cobalt district, Katanga, Democratic Republic of Congo. *In* Geology and genesis of major copper deposits and districts of the world: A tribute to Richard H. Sillitoe (J.W. Hedenquist, M.O. Harris, & F. Camus, eds.). *Society of Economic Geologists Special Publication* **16**, 269–301.

SELLEY, D., BROUGHTON, D., SCOTT, R., HITZMAN, M., BULL, S.W., LARGE, R.R., MCGOLDRICK, P.J., CROAKER, M., POLLINGTON, N., & BARRA, F. (2005) A new look at the geology of the Zambian Copperbelt. *In* Economic Geology 100th Anniversary Volume (J.W. Hedenquist, J.F.H. Thompson, R.J. Goldfarb, & J.P. Richards, eds.). Society of Economic Geologists,Colorado, United States (965–1000).

SHANNON R.D. (1976) Revised effective ionic radii and systematic studies of interatomic distances in halides and chalcogenides. *Acta Crystallographica* **A32**, 751–767.

SHEDD, K. (2013) Cobalt. *U.S.G.S. Mineral Commodity Summaries*, January 2013, 46–48.

SIMMONDS, J.R. (1980) *Significance of the Baluba orebodies with respect to Zambian copper-cobalt mineralization*. Unpublished Ph.D. thesis, University of Wales, 477p.

SWEENEY, M., TURNER, P., & VAUGHAN, D.J. (1986) Stable isotope and geochemical studies of the role of early diagenesis in ore formation, Konkola Basin, Zambian Copper Belt. *Economic Geology* **81**, 1838–1852.

VAN LANGENDONCK, S., MUCHEZ, P., DEWAELE, S., KAPUTO KALUBI, A., & CAILTEUX, J. (2013) Petrographic and mineralogical study of the sediment-hosted Cu–Co ore deposit at Kambove West in the central part of the Katanga Copperbelt (DRC). *Geologica Belgica* **16**, 91–104.

WARREN, J. (2000) Dolomite: occurrence, evolution and economically important associations. *Earth-Science Reviews* **52**, 1–81.

WHYTE, R.J. & GREEN, M.E. (1971) Geology and palaeogeography of Chibuluma West Orebody, Zambian Copperbelt. *Economic Geology* **66**, 400–424.

Received January 15, 2014, revised manuscript accepted August 5, 2014.